

## Article

# Interplay of Interfacial and Rheological Properties on Drainage Reduction in CO<sub>2</sub> Foam Stabilised by Surfactant/Nanoparticle Mixtures in Brine

Beatriz Ribeiro Souza de Azevedo <sup>1,2</sup>, Bruno Giordano Alvarenga <sup>1</sup>, Ana Maria Percebom <sup>2</sup>  
and Aurora Pérez-Gramatges <sup>1,2,\*</sup>

<sup>1</sup> Laboratory of Physical-Chemistry of Surfactants (LASURF), Pontifical Catholic University of Rio de Janeiro, Rio de Janeiro 22451-900, Brazil

<sup>2</sup> Department of Chemistry, Pontifical Catholic University of Rio de Janeiro, Rio de Janeiro 22451-900, Brazil

\* Correspondence: [aurora@puc-rio.br](mailto:aurora@puc-rio.br)

**Abstract:** Although nanoparticles (NPs) are known to increase foam stability, foam stabilisation is not observed in all surfactant/NP combinations. The present study evaluates the stability of CO<sub>2</sub> foams containing surfactant/NP mixtures with attractive or repulsive electrostatic interactions at the low pH imposed by CO<sub>2</sub> in the presence of a high-salinity brine. Three ionic surfactants and two oxide NPs (SiO<sub>2</sub> and Al<sub>2</sub>O<sub>3</sub>) were used in combinations of similar or opposite charges. Surface tension, viscosity,  $\zeta$ -potential and hydrodynamic size experiments allowed the analysis of CO<sub>2</sub> foam stability based on the impact of surfactant–NP interactions on bulk and interfacial properties. All oppositely charged systems improved the foam half-life; however, a higher NP concentration was required to observe a significant effect when more efficient surfactants were present. Both bulk viscosity and rigidity of the interfacial films drastically increased in these systems, reducing foam drainage. The mixture of SiO<sub>2</sub> with a zwitterionic surfactant showed the greatest increase in CO<sub>2</sub> foam stability owing to the synergy of these effects, mediated by attractive interactions. This study showed that the use of NPs should be tailored to the surfactant of choice to achieve an interplay of interfacial and rheological properties able to reduce foam drainage in applications involving CO<sub>2</sub> foam in brine.

**Keywords:** viscosity; foam; stability; salt; silica; alumina; surfactant; drainage rate

**Citation:** Azevedo, B.R.S.; Alvarenga, B.G.; Percebom, A.M.; Pérez-Gramatges, A. Interplay of Interfacial and Rheological Properties on Drainage Reduction in CO<sub>2</sub> Foam Stabilised by Surfactant/Nanoparticle Mixtures in Brine. *Colloids Interfaces* **2023**, *7*, 2. <https://doi.org/10.3390/colloids7010002>

Academic Editors: Marzieh Lotfi, Reinhard Miller and Mohammad Firoozzadeh

Received: 1 November 2022

Revised: 24 December 2022

Accepted: 3 January 2023

Published: 5 January 2023



**Copyright:** © 2023 by the authors. Licensee MDPI, Basel, Switzerland. This article is an open access article distributed under the terms and conditions of the Creative Commons Attribution (CC BY) license (<https://creativecommons.org/licenses/by/4.0/>).

## 1. Introduction

CO<sub>2</sub> foam has potential applications in controlling gas mobility in enhanced oil recovery (EOR) and mitigating carbon dioxide emissions. However, the high solubility of CO<sub>2</sub> in water results in fast foam coarsening and, consequently, in the early destruction of CO<sub>2</sub> foams [1,2]. Furthermore, the presence of salt in the aqueous phase, such as in brines that are commonly used in industrial applications, reduces the electric double layer around bubbles, thereby decreasing the repulsive forces and increasing the coalescence rate [3,4].

Surfactants are usually used as foam stabilisers; however, their rapid adsorption/desorption at fluid interfaces hinders the formation of a robust interfacial barrier that can reduce CO<sub>2</sub> diffusion from bubbles [5]. This effect can be compensated with the use of nanoparticles (NPs), because the high energy of attachment of particles to interfaces, relative to the thermal energy  $kT$ , promotes irreversible adsorption [6], thereby creating a physical barrier around the bubbles that delays foam coarsening and coalescence [7–9]. Moreover, the presence of NPs can increase the viscosity of the aqueous phase, thus further retarding foam destruction processes [10–12]. These effects are governed by particle–

particle interactions in the solution (structuring) and can be modulated by the presence of surfactants [13]. Therefore, the use of solid NPs to increase the stability of surfactant foams has attracted increased interest in foam-based EOR methods [14]. For example, when compared with the use of surfactants alone, the use of silica ( $\text{SiO}_2$ ) and alumina ( $\text{Al}_2\text{O}_3$ ) NPs combined with surfactants for the stabilisation of  $\text{CO}_2$  foam resulted in an approximately fivefold increase in the foam half-life [15]. Research on the effects of surfactants and NP types has indicated that the electrostatic attraction between the surface charge of the NPs and that of surfactant head groups plays a vital role in stabilising the foam [16]. These attractive interactions lead to enhanced NP adsorption at the gas–liquid interface and tighter packing at the lamellae, thereby slowing down the liquid drainage and enhancing foam stability.

Despite the reported advantages of incorporating solid particles into surfactant-stabilised aqueous foams, their influence on the formation and stability of the foam strongly depends on the surfactant type, and particle size and concentration. For instance, some researchers have stated that any NP can be used to stabilise surfactant foams [15,16]. However, a careful analysis of the literature shows that not all surfactant/NP combinations enhance the foam stability [17–20]. Therefore, the specific mechanisms mediated by surfactant/NP affinities, such as the effect on increasing mechanical strength of the lamellae, capillary pressure, and network structure formation, need to be better understood [21,22]. In particular, the choice of ionic surfactants, in combination with NPs exhibiting acid/base properties, for use in the stabilisation of  $\text{CO}_2$  foams remains a major research problem, because an acidic aqueous phase can have additional effects on the interactions in the bulk and at the bubble interface.

The present study aims to investigate the specific mechanisms involved in the stabilisation of  $\text{CO}_2$  foams by surfactant/NP mixtures that can present attractive or repulsive electrostatic interactions at the low pH imposed by the gas and in the presence of a high-salinity brine. To this end, we use three ionic surfactants with the same alkyl chain (C12) and different polar heads and two oxide NPs ( $\text{SiO}_2$  and  $\text{Al}_2\text{O}_3$ ) that exhibit opposite surface charges at the typical pH of  $\text{CO}_2$ -saturated aqueous solutions. The foam stability results are first analysed considering the impact of the surfactant–NP interactions in each system on the fluid properties (i.e., surface tension and viscosity) and the colloidal behaviour of NPs (i.e.,  $\zeta$ -potential and hydrodynamic size). The findings are then correlated with the specific mechanisms for arresting drainage in this type of foam, and the broader implications for the design of surfactant/NP mixtures in  $\text{CO}_2$  foam applications are discussed.

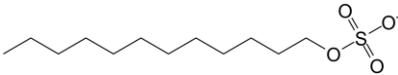
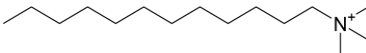
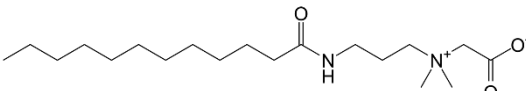
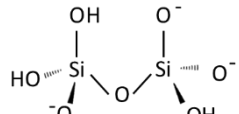
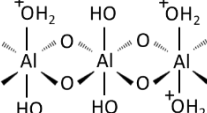
## 2. Materials and Methods

### 2.1. Materials

Three ionic surfactants with the same alkyl chain (C12) were used to evaluate the influence of charges on foam stabilisation: a negatively charged surfactant (sodium dodecyl sulphate, SDS, purity: 99%), a positively charged surfactant (dodecyl trimethyl ammonium bromide, DTAB, purity: 99%), and a zwitterionic surfactant (cocamidopropyl betaine, CAPB, activity: 99%) which exhibits both charges depending on the pH (isoelectric point 4.0 [23]). SDS and DTAB were purchased from Sigma-Aldrich (São Paulo, Brazil) and CAPB was kindly donated by Oxiteno (São Paulo, Brazil). These surfactants were used without further purification, and their working concentrations were determined based on the content of the active compound (purity) in the sample.

The NPs were selected based on their point of zero charge (pzc) to obtain different surface charges at the working pH (~5). The two oxide NPs used were  $\text{SiO}_2$  (pzc ~2) and  $\text{Al}_2\text{O}_3$  (pzc ~9) [24], obtained from Sigma-Aldrich (São Paulo, Brazil). They have similar primary particle sizes (12 and 13 nm, respectively). The molecular structures of the surfactants and NPs are shown in Table 1.

**Table 1.** Chemical names and structures of the surfactants and nanoparticles used in this work.

Chemical Name	Molecular Structure	CAS
Sodium dodecyl sulphate (SDS)		151-21-3
Dodecyl trimethyl ammonium bromide (DTAB)		1119-94-4
Cocamidopropyl betaine (CAPB)		61789-40-0
Silicon oxide (SiO <sub>2</sub> ) NP		7631-86-9
Alumina oxide (Al <sub>2</sub> O <sub>3</sub> ) NP		1344-28-1

Synthetic desulphated saline water containing the salts NaCl, CaCl<sub>2</sub>·2H<sub>2</sub>O, MgCl<sub>2</sub>·6H<sub>2</sub>O, KCl, Na<sub>2</sub>SO<sub>4</sub>, and NaHCO<sub>3</sub> (all obtained from Sigma-Aldrich, São Paulo, Brazil; purity > 98%) was used as the base aqueous fluid for the foaming formulations (Table 2). The composition of this brine was similar to that of desulphated seawater commonly used for injection in offshore EOR projects in Brazil [25]. Ultrapure water obtained from a Milli-Q Direct 8 system (18.2 MΩ cm at 25 °C) was used in all the preparations. The CO<sub>2</sub> gas (purity: 99.5%) used for foam production and pH adjustment was purchased from Linde Gas (Rio de Janeiro, Brazil).

**Table 2.** Composition of the brine (synthetic desulphated saline water) used in the formulation of aqueous fluids.

Ion	Concentration (mg L <sup>-1</sup> )
Na <sup>+</sup>	22,016
Ca <sup>2+</sup>	264
Mg <sup>2+</sup>	302
K <sup>+</sup>	786
SO <sub>4</sub> <sup>2-</sup>	78
Cl <sup>-</sup>	35,873
HCO <sub>3</sub> <sup>-</sup>	72

## 2.2. Experimental Procedures

### 2.2.1. Preparation of Surfactant Solutions and NP Dispersions

Surfactant solutions were prepared at 0.1 wt % by dissolving appropriate surfactant amounts or by diluting commercial formulations into desulphated seawater brine (composition in Table 2). The surfactant solutions were stirred for at least 1 h at room temperature (25 °C) using a magnetic stirrer. The NP dispersions were prepared by dispersing appropriate amounts into brine or 0.1 wt % surfactant solutions to achieve the desired concentration. The NP were compared at the same concentration in wt % despite their difference in specific gravity to enable comparisons with relevant previous studies that used such NPs. The dispersions were first mixed for 1 h by using a magnetic stirrer and then sonicated using an ultrasonic bath for 20–30 min. For the non-foaming experiments,

CO<sub>2</sub> was first bubbled into the solution to resemble the working pH of the aqueous phase during foaming.

### 2.2.2. Foam Characterisation

Foam decay curves were obtained using a dynamic foam analyser (DFA100) from Kruss, with a glass column measuring 40 mm in diameter. CO<sub>2</sub> foam was generated by bubbling the gas through a porous membrane (diameter: 30 mm; pore size: 15–25 µm) into 50 mL of surfactant or surfactant/NP in brine. The gas flow rate was set at 0.5 L min<sup>-1</sup> and was interrupted when the foam reached a height of 200 mm. All foams were evaluated at least two times using independent surfactant solutions. The concentration of the surfactants was fixed at 0.1 wt %, which is the lower limit of the concentration range typically used in CO<sub>2</sub> foam field applications. Two NP concentrations, 0.5 wt % and 1.0 wt %, were used.

The foaming factor (*FF*), defined as the volume of generated foam divided by the volume of gas used during foam formation, was calculated to compare the foamabilities of the systems. The volumes of foam (*V<sub>f</sub>*) and liquid (*L*: volume of liquid at a given time; *L<sub>F</sub>*: maximum liquid volume) were obtained by measuring their respective heights in the column using a 469 nm light source with 20% luminosity. The half-life of the foam (*t<sub>1/2</sub>*), defined as the time required for the foam column to decay to half its initial height, was used as the criterion for foam stability. In addition, the relative half-life (*t<sub>1/2</sub><sup>rel</sup>*) was calculated as the ratio of the half-lives of the surfactant/NP and surfactant-only foams. The liquid content (*ε*) was defined as the ratio of the liquid volume in the foam and the total foam volume, with *ε<sub>0</sub>* being the ratio immediately after foam formation. The initial drainage rate (*DR<sub>i</sub>*) was obtained by plotting the normalised volume of the drained liquid (*L/L<sub>F</sub>*) over time. The initial slopes obtained by linear fitting represent *DR<sub>i</sub>*.

### 2.2.3. Surface Tension

Surface tension (*γ*) measurements were performed using a Kibron EZ Pl-Plus tensiometer at 25 °C by the Wilhelmy method (standard deviation < 0.01 mN m<sup>-1</sup>). A plot of the surface tension (*γ*) versus the surfactant concentration (*log C<sub>surf</sub>*) was used to determine the minimum surface tension (*γ<sub>min</sub>*), CMC, surface excess concentration (*Γ*), and surface area per molecule (*A<sub>m</sub>*). The CMC was determined as the surfactant concentration at which a discontinuity was observed in the surface tension plot [26]. The *Γ* was obtained from the Gibbs adsorption equation (Equation (1)), where *R* is the universal gas constant and *T* is the temperature (in Kelvin). The area occupied by a surfactant molecule in the monolayer at the surface is given by *A<sub>m</sub>* = 1/(*N<sub>A</sub>* × *Γ*), where *N<sub>A</sub>* is Avogadro's number [26].

$$\Gamma = \frac{-1}{2RT} \left( \frac{\partial \gamma}{\partial C_{surf}} \right)_{T,p} \quad (1)$$

Additionally, the surface tension data were used to evaluate *pC<sub>20</sub>*, which indicates the efficiency of adsorption of the surfactant (negative log of the minimum concentration of the surfactant in bulk required to produce maximum adsorption at the interface) [26]. The parameter *pC<sub>20</sub>* was calculated as the logarithm of the surfactant concentration required to reduce the surface tension of aqueous solutions by 20 mN m<sup>-1</sup>.

In the case of the surfactant/NP systems, the surface tension of the aqueous phase was measured after CO<sub>2</sub> foam formation. All surface tension measurements were performed in triplicate.

### 2.2.4. Viscosity

The variation in the viscosity with the shear rate (flow curves) of the surfactant solutions and surfactant/NP dispersions was evaluated using a HAAKE MARS 60 rheometer equipped with a double-gap cell (volume: 3 mL; gap: 4 mm). Initially, all samples were subjected to pH adjustment by bubbling with CO<sub>2</sub> for 2 min. The formulations containing NPs were placed in an ultrasonic bath for 10 min before measurements in the rheometer.

The samples were allowed to stand for 10 min in the rheometer before the measurement to equilibrate the temperature. The temperature was set to 25 °C using an external water bath system with a precision of 0.1 °C. Flow curves were obtained over a shear rate range of 0.01–1000 s<sup>−1</sup>. The experiments were performed in triplicate, with independent solutions.

### 2.2.5. Dynamic Light Scattering

Dynamic light scattering (DLS) measurements were performed at 25 °C to obtain the NP hydrodynamic diameter ( $D_H$ ) in brine, in the absence and presence of surfactants; these measurements were performed using a Zetasizer Nano ZS (Malvern Instruments, Worcestershire, U.K.) equipped with a He-Ne laser at 633 nm. A polystyrene cuvette with polished walls (DTS0012) was used. The tests were performed in triplicate, with durations defined in automatic mode (a minimum of 10 and a maximum of 100 runs), backscattering configuration ( $\theta = 173^\circ$ ), and at 25 °C. In addition, the charges were evaluated via  $\zeta$ -potential measurements using the same equipment under identical conditions. The Smoluchowski equation was used to convert the electrophoretic mobility into surface charge values. The dispersions of NPs (0.01 wt %) were evaluated in ultrapure water and surfactant solutions (0.1 wt %) in brine using a high concentration  $\zeta$ -potential cell (ZEN1010, Malvern Instruments, Malvern Worcestershire, U.K.). The final pH of all dispersions was approximately 5 owing to previous saturation with CO<sub>2</sub> (resembling foaming conditions).

## 3. Results

### 3.1. CO<sub>2</sub> Foam Behaviour of Cationic, Anionic, and Zwitterionic Surfactants in Brine

The CO<sub>2</sub> foam behaviour of the brine formulations containing only surfactants was analysed by considering the interfacial properties of the surfactant. The foam decay profiles of SDS and CAPB were very similar, and the foam stability of both surfactants was higher than that of the foam stabilised with DTAB, a cationic surfactant of the same chain length (Figure 1). The poorer foam stabilisation performance of DTAB in comparison with SDS has been reported for nitrogen foams [27,28].

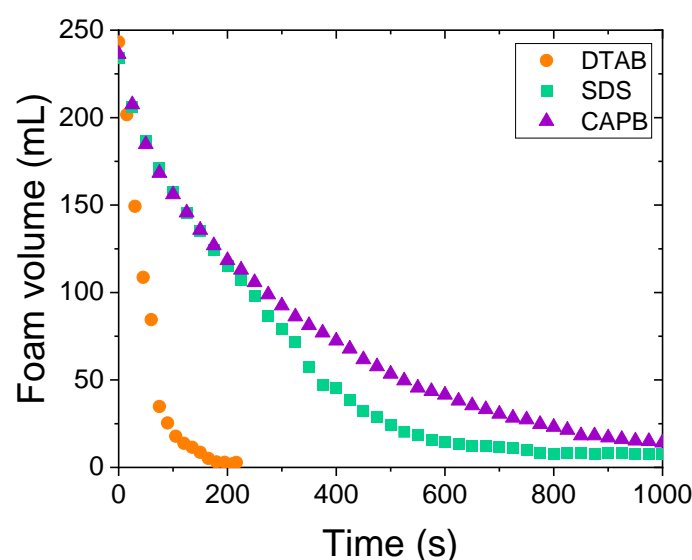


**Figure 1.** Foam decay profiles of CO<sub>2</sub> foam formed with 0.1 wt % surfactant-only formulations, in desulphated seawater brine at 25 °C (standard deviation: foam height < 5 mL).

Conversely, the nature of the ionic head did not significantly affect the foamability ( $FF$ ); this can be explained by the minimum critical surface tension ( $\gamma_{min}$ ), which was in the range of 30–40 mN m<sup>−1</sup> for all surfactants (Table 3). This reduction in the surface tension was sufficient to create new interfaces when bubbles were generated. The marginally

smaller  $FF$  value of DTAB was attributed to the higher  $\gamma_{min}$  than that of the other surfactants, which could have contributed to faster foam destruction during  $\text{CO}_2$  foam formation.

**Table 3.** Interfacial and  $\text{CO}_2$  foam properties of surfactant formulations in brine ( $FF$ : foaming factor,  $t_{1/2}$ : foam half-life,  $\gamma_{min}$ : minimum surface tension,  $\Gamma$ : surfactant excess concentration,  $A_m$ : mean area per surfactant molecule at the interface, CMC: critical micelle concentration,  $pC_{20}$ : adsorption efficiency).

Surfactant	Foaming		Interfacial				
	$FF$	$t_{1/2}$ (s)	$\gamma_{min}$ (mN m <sup>-1</sup> )	$\Gamma$ (mol m <sup>-2</sup> )	$A_m$ (Å <sup>2</sup> molecule <sup>-1</sup> )	CMC (wt %)	$pC_{20}$
SDS	0.55	196	31.3	$4.29 \times 10^{-6}$	38.7	0.01	3.1
DTAB	0.51	39	38.1	$4.44 \times 10^{-6}$	37.4	0.05	2.0
CAPB	0.56	201	35.3	$6.54 \times 10^{-6}$	25.4	0.002	3.4

Further analysis using the half-life ( $t_{1/2}$ ) of the foams showed that the differences observed in foam stability could not be correlated with the CMC of the surfactants in brine (Table 2). The CMC of the zwitterionic surfactant was an order of magnitude lower than that of the anionic and cationic surfactants. However,  $t_{1/2}$  of CAPB was very similar to that of SDS, and the DTAB foam exhibited a much shorter time. A similar analysis using  $A_m$  indicated that the interfacial films formed by the anionic and cationic surfactants at the gas–water interface had similar packing. A better correlation was observed with  $pC_{20}$ , which is related to the free energy change involved in the adsorption of the surfactant at the interface [26]. Both CAPB and SDS showed similar  $pC_{20}$  values which were greater than that of DTAB, indicating that these surfactants are more efficient at stabilising the interface, as reflected in the highest stability of their foams over time. The greater the  $pC_{20}$  value, the larger is the  $\Delta G_0$  value for transferring a surfactant molecule from the bulk to the interface, and this process is thermodynamically favoured. Therefore, because the increase in the surfactant adsorption efficiency at the gas–water interface promotes stabilisation via the Marangoni effect [29], the bubble elasticity increased in systems containing anionic and zwitterionic surfactants, which can be related with the greater foam stability observed.

### 3.2. Effect of $\text{SiO}_2$ and $\text{Al}_2\text{O}_3$ NPs on Foam Stability

The influence of NP surface charges on the stability of  $\text{CO}_2$  foam with formulations containing surfactant/NP mixtures was studied using two oxide NPs with similar nominal sizes (to avoid the effects of initial NP size) and at two NP concentrations. The aqueous phase in this type of foam is characterised by a low pH (~5, Table S1 in Supplementary Materials) owing to the dissolution of  $\text{CO}_2$  during foam formation. At this pH, the surface charges of the  $\text{SiO}_2$  and  $\text{Al}_2\text{O}_3$  NPs were −10 mV and +23 mV, respectively (Table S3 in Supplementary Materials), allowing both NPs to interact with attractive or repulsive electrostatic interactions according to the surfactant head group.

The results showed a general trend of significant improvement in  $\text{CO}_2$  foam stability in systems containing oppositely charged groups, that is, DTAB/ $\text{SiO}_2$  and SDS/ $\text{Al}_2\text{O}_3$  (Figure 2a–d). The influence of electrostatic attraction has been shown to be dominant in promoting foam stability [16]; at the same time, some reports note that similarly charged components contribute to reducing foam destruction [30]. In the present study, a marginal increase in the foam stability was observed for the SDS/ $\text{SiO}_2$  system (1.0 wt %), where both the surfactant and NP exhibit negative charges (Figure 2c). This behaviour can be attributed to the possible weak hydrophobic interactions between the surfactant hydrocarbon chains and  $\text{SiO}_2$  NP surface groups [31,32].

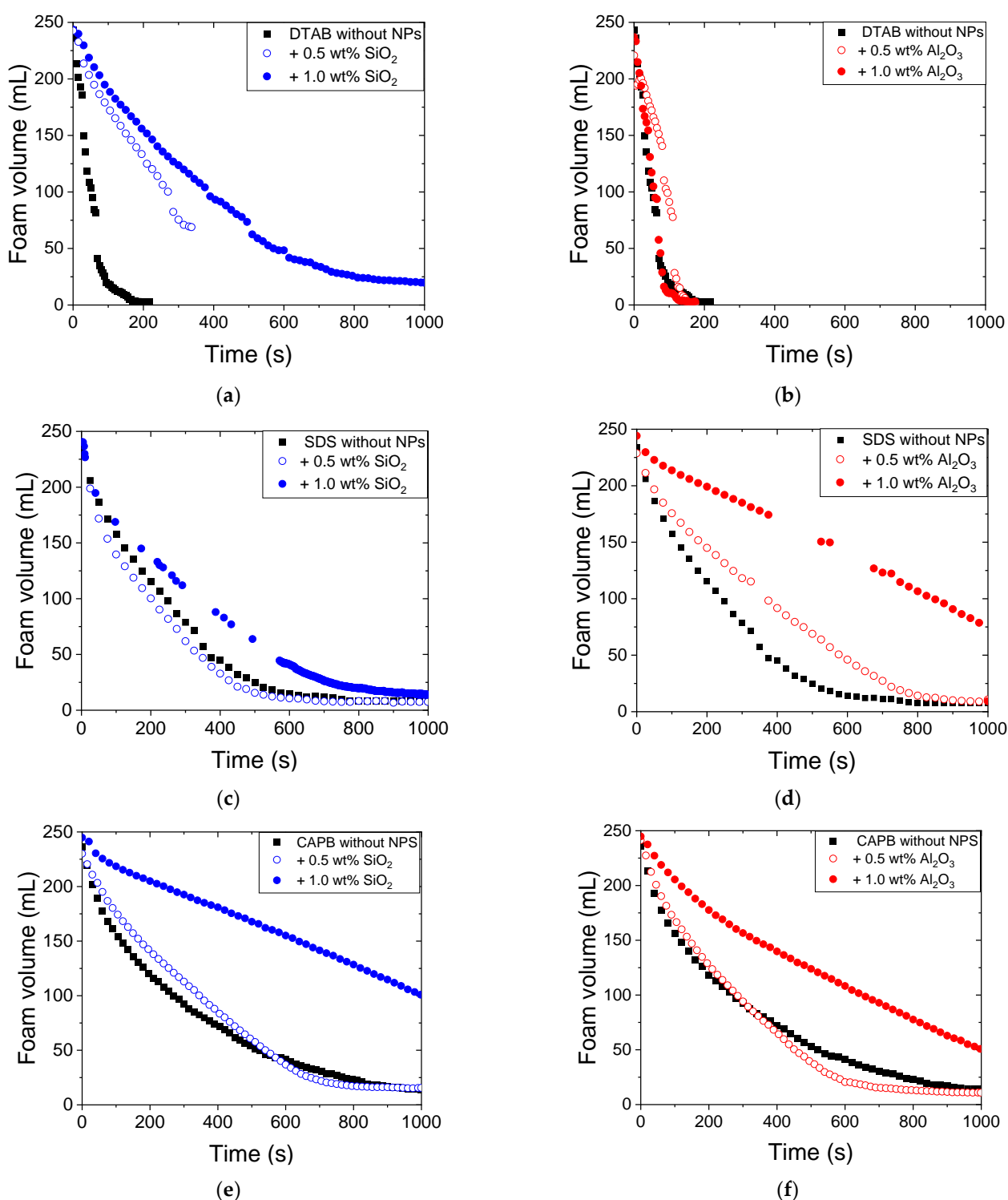


**Figure 2.** Foam decay profiles of CO<sub>2</sub> foam formed for 0.1 wt % (a,b) DTAB, (c,d) SDS, and (e,f) CAPB in the absence and presence of NPs (in brine at 25 °C) (standard deviation: foam volume <5 mL).

These results partially agree with those reported by Yekeen et al. [33], wherein the stability of CO<sub>2</sub> foams containing SDS increased with an increase in the concentrations of SiO<sub>2</sub> and Al<sub>2</sub>O<sub>3</sub> NPs up to 1.0 wt %. However, the study by Yekeen et al. did not detect any differences between the effects of SiO<sub>2</sub> and Al<sub>2</sub>O<sub>3</sub> NPs on the stabilisation of CO<sub>2</sub> foams containing SDS.

The improvement in CO<sub>2</sub> foam stability in oppositely charged systems did not follow the same trend with increasing NP concentration. The foams formed with the cationic surfactant exhibited a drastic increase in stability in the presence of only 0.5 wt % SiO<sub>2</sub> NPs, and a further increase in the NP concentration only led to a discrete effect. Conversely, the greatest improvement in the foam stability with anionic surfactants was obtained with 1.0 wt % of Al<sub>2</sub>O<sub>3</sub> NPs, suggesting that the effect of adding NPs in these systems also depends on the foaming properties of the surfactant. In the latter system, a higher NP concentration was needed for a significant improvement because SDS is already an efficient foamer (Figure 1). In contrast, systems such as DTAB, which contain a poorer foamer, can benefit from lower NP concentrations. In addition, the CO<sub>2</sub> foam stability of the SDS/Al<sub>2</sub>O<sub>3</sub> system at 1.0 wt % NP concentration was significantly higher than that of DTAB/SiO<sub>2</sub> (Figure 2a,d), indicating that there might be a limit on the improvement in foam stability owing to the addition of NPs in systems based on surfactants with poor foaming properties.

These hypotheses were confirmed by the behaviour observed in the CO<sub>2</sub> foams formulated with the zwitterionic surfactant, where an improvement in the foam stability was obtained in the presence of both NPs, but only at the highest concentration (Figure 2e,f). The presence of both charges in the surfactant molecule at the working pH of the aqueous phase (CAPB isoelectric point: 4.0 [23]) allowed for strong attractive surfactant–NP interactions in both systems, leading to improved foam stabilisation. However, the effect was negligible at 0.5 wt % NP concentration, confirming that for surfactants with adequate foaming properties, higher NP concentrations are required to achieve significant benefits towards CO<sub>2</sub> foam stabilisation. Moreover, high NP concentrations are necessary for significant stabilisation of these CO<sub>2</sub> foams owing to the large gas solubility in the aqueous phase, in contrast to results reported for N<sub>2</sub> foams, in which lower NP concentrations (0.1 wt %) were required [34].

### *3.3. Interfacial, Colloidal, and Rheological Properties of Surfactant/NP Systems: Implications for foam Destabilisation*

To examine the role of surfactant–NP interactions on the CO<sub>2</sub> foam stability in these systems, the bulk and interfacial properties of the aqueous NP dispersions were determined and discussed in terms of the foam destabilisation mechanisms. The dispersions were prepared at 1.0 wt % NP concentration because the most significant differences in the behaviour were observed at this concentration.

The viscosity of fluids containing NPs is known to be notably higher than that of dilute surfactant solutions [13]. All the surfactant/NP formulations in this study showed an increase in viscosity and exhibited non-Newtonian behaviour. In contrast, the surfactant solutions behaved as Newtonian fluids, in a manner similar to the aqueous brine (Figure 3a). This behaviour is characteristic of colloidal dispersions as a result of rearrangements of the NPs in the bulk (alignments on the flow) with the applied shear [35]. All samples exhibited shear thinning behaviour; in other words, the viscosity decreased with increasing shear rate, and the viscosity was higher than that in the absence of NPs even at high shear rates. This increase in the viscosity was more pronounced in systems containing oppositely charged surfactant/NP pairs than in those with the same charge. To further explore this effect, the viscosities of the surfactant/NP systems were compared at a shear rate of 10 s<sup>−1</sup>, relative to their values without NPs (Figure 3b). This shear rate was selected within the local shear rate range observed in foam films formed with non-Newtonian fluids of similar viscosity by Safoune et al. [36]. As can be seen, the highest viscosities for each surfactant corresponded to the systems containing NPs with opposite charges, including the two CAPB formulations. This behaviour agrees well with the highest values of foam half-life ( $t_{1/2}$ , Table 3) obtained from the foam decay curves and confirms the importance of the viscosity of the aqueous phase in the stability of CO<sub>2</sub> foams. Previous studies from our group [37,38] and others [39–41] have also shown the relevance of increasing



the viscosity of the aqueous phase in obtaining a significant improvement in CO<sub>2</sub> foams in brine.

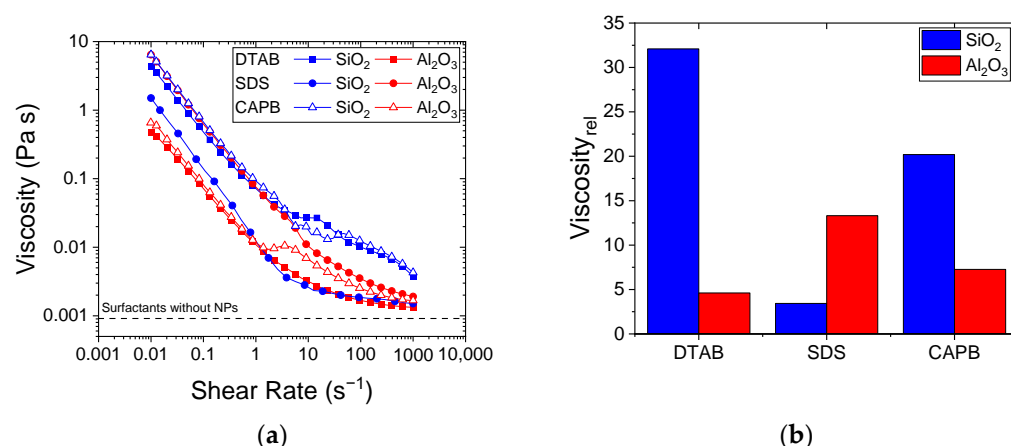


**Figure 3.** (a) Flow curves of solutions containing DTAB, SDS, or CAPB in the presence of 1.0 wt % NPs and (b) their relative viscosities (ratio of viscosities with and without NPs) at a shear rate of 10 s<sup>-1</sup>.

However, the viscosity values did not show a direct correlation with the foam half-life: DTAB/SiO<sub>2</sub> had the highest viscosity, whereas CAPB/SiO<sub>2</sub> showed the longest foam  $t_{1/2}$  (846 s). A better correspondence was found considering the relative foam half-life ( $t_{1/2}^{rel}$ , Table 4), that is, the improvement in foam stability with NPs compared to the surfactant-only foam. The parameter  $t_{1/2}^{rel}$  shows the direct impact of the increase in viscosity due to the presence of NPs on reducing CO<sub>2</sub> foam decay because all oppositely charged systems followed the same order: DTAB/SiO<sub>2</sub> > CAPB/SiO<sub>2</sub> > SDS/Al<sub>2</sub>O<sub>3</sub> > CAPB/Al<sub>2</sub>O<sub>3</sub>. This behaviour confirms the importance of the viscosity of the aqueous phase on the CO<sub>2</sub> foam stability, which can compensate for the poor foaming properties of surfactants such as DTAB.

**Table 4.** Half-life ( $t_{1/2}$ ) and relative half-life ( $t_{1/2}^{rel}$ ) of CO<sub>2</sub> foams containing surfactants and NPs (1.0 wt %) in desulphated seawater brine.

Surfactant/NP	DTAB			SDS			CAPB		
	Without NP	SiO <sub>2</sub>	Al <sub>2</sub> O <sub>3</sub>	Without NP	SiO <sub>2</sub>	Al <sub>2</sub> O <sub>3</sub>	Without NP	SiO <sub>2</sub>	Al <sub>2</sub> O <sub>3</sub>
CO <sub>2</sub> foam $t_{1/2}$ (s)	39	250	50	196	265	737	201	846	511
CO <sub>2</sub> foam $t_{1/2}^{rel}$		6.4	1.0		1.4	3.7		4.1	2.5

The viscosity of the aqueous phase in NP dispersions is directly related to their colloidal properties [30]. Therefore, the changes in NP surface charges upon their dispersion in the surfactant formulations were analysed to examine the type and extent of interactions in the surfactant/NP systems studied herein. The  $\zeta$ -potentials of SiO<sub>2</sub> and Al<sub>2</sub>O<sub>3</sub> NPs showed significant variations in the presence of DTAB (from −10 mV to +20 mV) and SDS (from +23 mV to −33 mV), respectively, owing to surfactant adsorption on oppositely charged surfaces (Figure 4a, Table S2 in Supplementary Materials). However, in systems bearing the same type of charge, the changes in the  $\zeta$ -potential were negligible ( $\Delta\zeta \leq 5$  mV). The large surfactant adsorption on the NP surface was confirmed by the inversion of the charge sign in the systems with attractive interactions: the charge sign changed from negative to positive in SiO<sub>2</sub> NP upon the adsorption of DTAB, and from positive to negative in Al<sub>2</sub>O<sub>3</sub> NPs upon SDS adsorption. The attractive electrostatic interactions in these systems, which are responsible for the increase in the colloidal stability of NPs in brine, can promote faster migration and adsorption of the NPs to the interface [42]. This effect was corroborated by the changes observed in the  $\gamma$  values in the surfactant/NP systems

compared to that of the surfactant-only solution (Figure 4b). The systems with larger variations in  $\zeta$ -potential evidently showed an increase in the interfacial tension, which can be related to the displacement of surfactant molecules by the adsorption of less surface-active NPs [42]. The presence of NPs at the interface confers more rigidity and elasticity to the bubble surfaces, thereby improving the stabilisation of the CO<sub>2</sub> foams (higher  $t_{1/2}$ ).

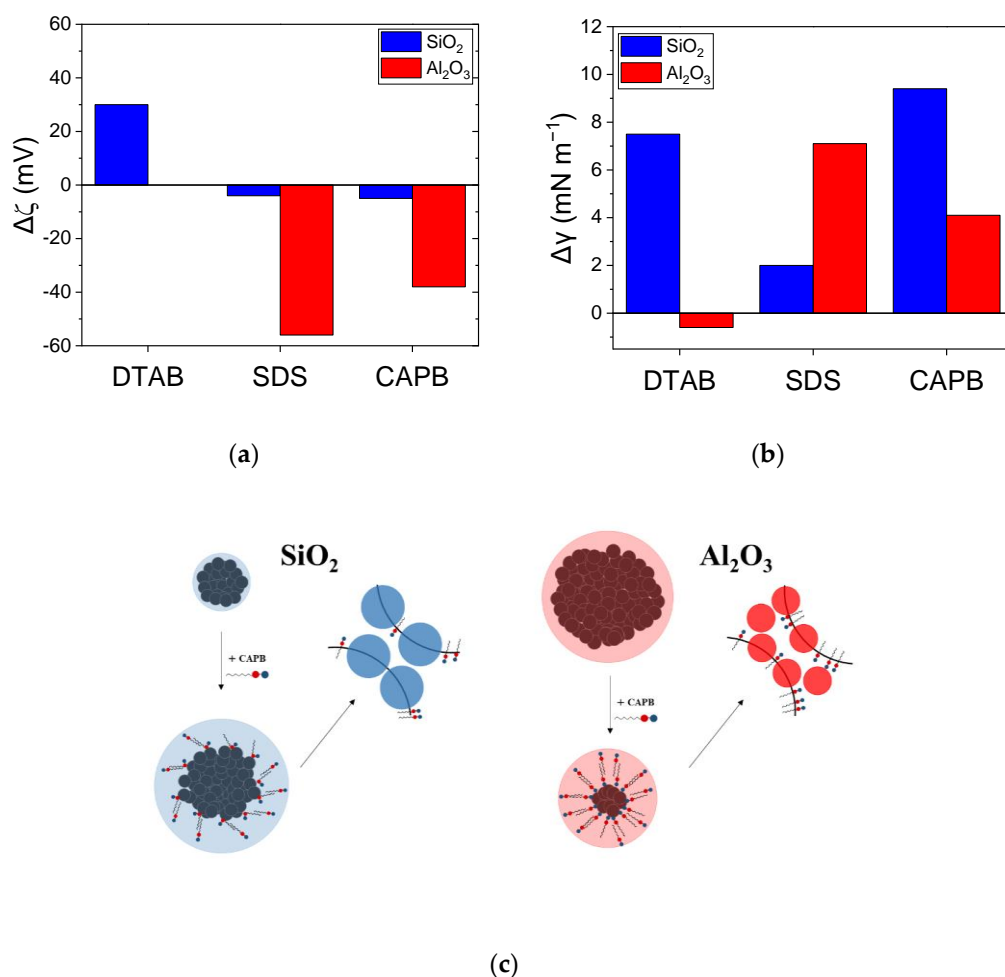


**Figure 4.** Changes in (a)  $\zeta$ -potential of NPs in the presence of surfactants, and in (b) surface tension ( $\gamma$ ) of the surfactant in the presence of NPs (formulations in desulphated seawater brine, at 25 °C). (c) Schematics illustrating the effect of the zwitterionic surfactant (CAPB) on NP dispersion in brine and adsorption at the gas–solution interface.

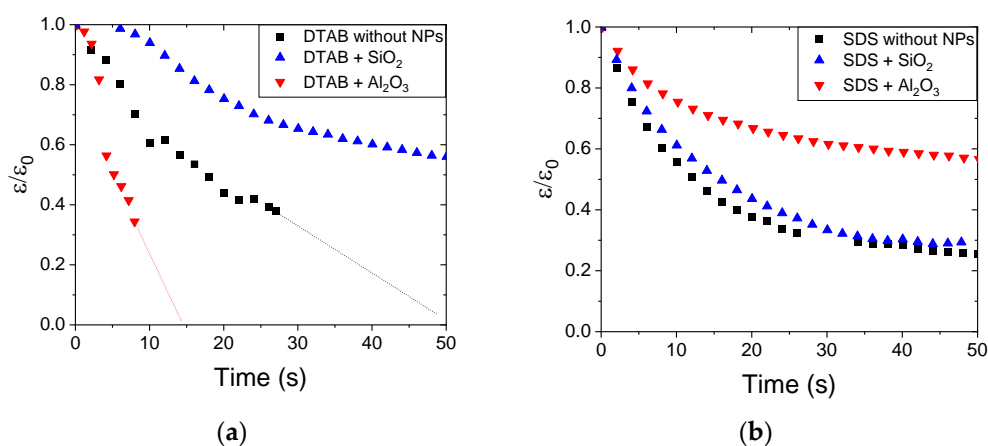
An intriguing behaviour was observed in the systems containing zwitterionic surfactants. Although the Al<sub>2</sub>O<sub>3</sub> NPs showed a significant change (and charge sign inversion) in the  $\zeta$ -potential when dispersed in CAPB, no significant change was observed for SiO<sub>2</sub> NP, indicating low surfactant adsorption on the NP surface. In contrast, this system exhibited the largest  $\Delta\gamma$  value, suggesting significant adsorption of NPs at the interface. To shed light on this contrasting behaviour, DLS was used to measure the hydrodynamic diameter ( $D_H$ ) of the aggregates formed by the NPs in brine and in the presence of CAPB (Figure S1 in Supplementary Materials). In brine, the  $D_H$  of aggregates of SiO<sub>2</sub> NPs ( $333 \pm 4$  nm) was smaller than that of Al<sub>2</sub>O<sub>3</sub> NPs ( $2515 \pm 4$  nm) because the effect of bivalent anions (SO<sub>4</sub><sup>2-</sup>) from brine on the electrical double layer is greater in Al<sub>2</sub>O<sub>3</sub> NPs. These divalent ions could create a bridge between the positive surface sites of Al<sub>2</sub>O<sub>3</sub> NPs, eliminating the electrostatic repulsion and, consequently, promoting an expressive increase in the hydrodynamic diameter [43]. In the presence of CAPB, this effect was mitigated by the formation

of a surfactant bilayer that stabilised the  $\text{Al}_2\text{O}_3$  NPs in the brine [44,45], and the NPs were better dispersed ( $D_H = 732 \pm 55$  nm). However, the opposite effect was observed for  $\text{SiO}_2$  NPs, wherein the  $D_H$  in CAPB solutions increased to  $2167 \pm 165$  nm, likely owing to the low  $\zeta$ -potential ( $-15$  mV, Table S3 in Supplementary Materials), and, in turn, resulting in NP aggregation. In this case, once the larger aggregates of  $\text{SiO}_2$  NPs adsorb at the bubble interfaces, they occupy a larger interfacial area and displace the surfactant molecules, thus explaining the increased interfacial tension in these systems (Figure 4c). Furthermore, these results can be correlated with the rheological transitions observed in the flow curves of these two systems (Figure 3a). In the CAPB/ $\text{Al}_2\text{O}_3$  system, where the inter-NP interactions in the solution become weaker (as  $D_H$  decreases), the rheological transition occurs at a lower shear rate than that in the CAPB/ $\text{SiO}_2$  system. The latter showed the same transition at a much higher shear rate, indicating that more energy was necessary to break the NP network in the solution [46], which was responsible for the high viscosity.

An analysis of the combination of the rheological and colloidal properties of the surfactant/NP brine formulations and the behaviour observed in  $\text{CO}_2$  foam stability indicates that the strong interactions occurring in oppositely charged systems are responsible for two main phenomena. The first is the formation of NP networks in the solution (as evidenced by the rheological transitions and the increase in the bulk viscosity). The second is the enhanced adsorption of NPs at the gas–solution interface (as evidenced by an increase in the surface tension). These two processes have been reported to delay main foam destruction mechanisms such as drainage and coarsening [47]. In the next section, we discuss more insights into the influence of these NP-mediated phenomena on foam drainage, and its implication for the stability of the  $\text{CO}_2$  foams studied in this work.

### 3.4. Impact of Drainage Mechanism in the Presence of NPs on Foam Half-Life

Coarsening is the most important mechanism in  $\text{CO}_2$  foams owing to the high gas diffusion. However, coarsening can be minimised by reducing the drainage because a greater volume of liquid contributes to thicker interbubble films and hinders gas diffusion [48,49]. The contribution of NPs in delaying foam destabilisation by controlling drainage can be evidenced by the trapping of liquid at the plateau borders via the formation of a rigid barrier in foam films [50]. The normalised liquid content ( $\varepsilon/\varepsilon_0$ ) was used as a parameter to quantify and compare the amount of liquid trapped in the  $\text{CO}_2$  foams studied herein. The variation in  $\varepsilon/\varepsilon_0$  with time showed that the liquid drainage was significantly reduced in foams with oppositely charged combinations (e.g., DTAB/ $\text{SiO}_2$  and SDS/ $\text{Al}_2\text{O}_3$ ) (Figure 5), along with the improved foam stability. In addition, a detailed analysis of the drainage time helped better understand the role of NPs in the stability of these foams. For example, in the SDS/ $\text{SiO}_2$  system, no significant reduction in the drainage was observed despite some improvement in the foam stability (Figure 2c). Furthermore, in the DTAB/ $\text{Al}_2\text{O}_3$  system, same-charge NPs accelerated foam drainage; that is, the presence of  $\text{Al}_2\text{O}_3$  with DTAB in the  $\text{CO}_2$  foam was detrimental to the foam stability, which could not be explained by the  $\text{CO}_2$  foam volume profiles alone (Figure 2b).



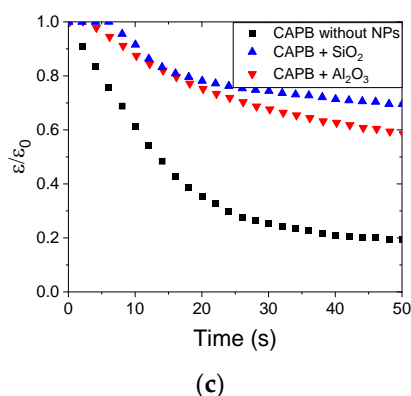


**Figure 5.** Normalised liquid content ( $\epsilon/\epsilon_0$ ) profiles with the time of CO<sub>2</sub> foams formed with (a) DTAB, (b) SDS, and (c) CAPB surfactants, in the absence and presence of 1.0 wt % SiO<sub>2</sub> or Al<sub>2</sub>O<sub>3</sub> (in desulphated seawater brine, at 25 °C).

A linear correlation was found between the foam half-life ( $t_{1/2}$ ) and drainage half-life ( $d_{1/2}$ ) of CO<sub>2</sub> foams in the presence of NPs for all systems, except for CAPB/SiO<sub>2</sub> which exhibited a much more pronounced delay in drainage (Figure 6a). However, despite the deceleration of drainage being directly related to the viscosity of the aqueous phase, the CAPB/SiO<sub>2</sub> system did not have the highest viscosity (Figure 6b). In fact, the most viscous fluid (DTAB/SiO<sub>2</sub>) resulted in a CO<sub>2</sub> foam with relatively low  $t_{1/2}$  and  $d_{1/2}$ . This suggests that the increase in viscosity due to NPs in oppositely charged systems cannot fully explain the observed CO<sub>2</sub> foam stability trends. Other effects discussed in the previous sections include the surfactant adsorption efficiency and the presence of adsorbed NPs at the gas–solution interface.

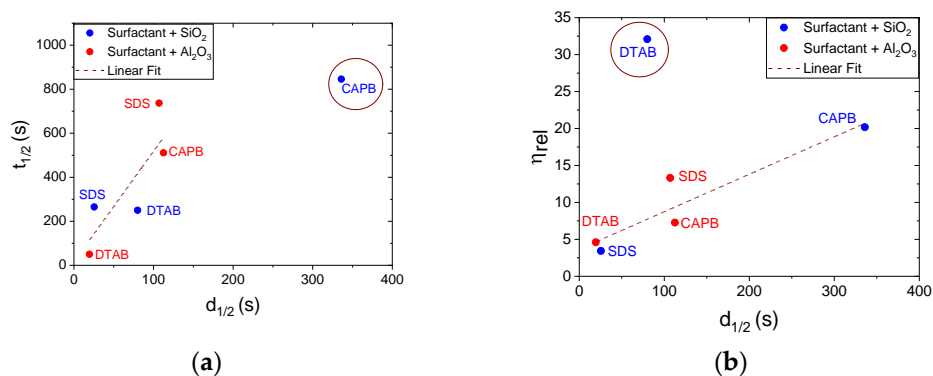


**Figure 6.** (a) Correlation between foam half-life ( $t_{1/2}$ ) and drainage half-life ( $d_{1/2}$ ). (b) Correlation between bulk relative viscosity ( $\eta_{rel}$ ) and drainage half-life ( $d_{1/2}$ ) of CO<sub>2</sub> foams formed with surfactants in the presence of 1.0 wt % NPs. (The lines are a guide for the eyes.).

In addition to the changes in surface tension, NP adsorption can alter the mechanical and rheological properties of the interfaces, which are key factors for foam stability. For example, immobile and rigid interfaces can reduce the drainage rate because fluid flow on the plateau border is Poiseuille-like [48]. Alternatively, when the interface is fluid and mobile, it flows with the bulk liquid and plug flow is observed. This indicates that a fluid interface provides significantly less resistance to the flow than a rigid interface [51]. Therefore, we can expect a greater deceleration of the drainage rate in systems with a larger amount of adsorbed NPs, which confers higher rigidity/immobility to the gas–liquid interfaces.

This effect was experimentally demonstrated by calculating the initial drainage rate ( $DR_i$ ) from the linear fits of the normalised drained liquid volume ( $L/L_F$ , see Figure S2 in Supplementary Materials) during the first 20 s after foam formation. During this early

stage of foam life, drainage can be considered the dominant mechanism because coarsening is not fast enough to cause a significant increase in the bubble curvature [51]. Figure 7 shows the effect of NPs in oppositely charged systems compared to that in the surfactant solutions:  $DR_i$  is reduced in the SDS/ $\text{Al}_2\text{O}_3$  and DTAB/ $\text{SiO}_2$  systems as well as in the two systems with zwitterionic surfactants. In these systems, the presence of NPs at the interface (greater  $\Delta\gamma$ ) confers more rigidity to the interface, thereby reducing the liquid flow. Conversely, the DTAB/ $\text{Al}_2\text{O}_3$  and SDS/ $\text{SiO}_2$  combinations exhibited faster initial drainage (high  $DR_i$ ). In these systems, the electrostatic repulsion between the surfactant and NPs of the same charge at the interface could make the interfacial film less rigid and more mobile, thereby accelerating the drainage process.

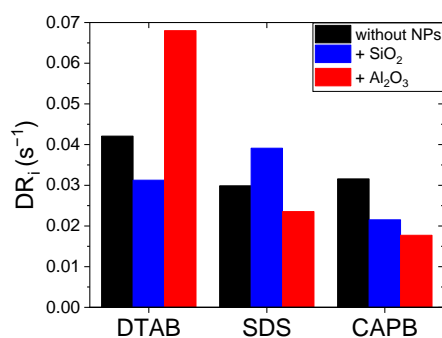


**Figure 7.** Initial drainage rate ( $DR_i$ ) of  $\text{CO}_2$  foams formed for DTAB, SDS, and CAPB, in the absence and presence of 1.0 wt %  $\text{SiO}_2$  or  $\text{Al}_2\text{O}_3$  (in desulphated seawater brine, at 25 °C).

Interestingly, although the combinations of  $\text{SiO}_2$  with DTAB and CAPB caused a similar  $DR_i$  reduction compared to that in the case of pure surfactants, the effect of the reduction in the drainage rate was much more pronounced in the system with the zwitterionic surfactant. This effect confirms that despite the increase in interfacial rigidity due to the presence of  $\text{SiO}_2$  NPs, the poor efficiency of DTAB regarding surfactant adsorption at interfaces (lower  $pC_{20}$ ) limited the overall  $\text{CO}_2$  foam stability. Similarly, the larger  $D_H$  of the  $\text{Al}_2\text{O}_3$  NPs in CAPB could be responsible for the greater increase in the interface rigidity (smaller  $DR_i$ ) compared with that in the SDS/ $\text{Al}_2\text{O}_3$  system. Therefore, for efficient foamers, the maximum increase in the  $\text{CO}_2$  foam stability can be achieved for NPs that strongly adsorb at the interfacial film and subsequently generate a rigid immobile surface and produce a significant increase in the bulk viscosity, such as in the CAPB/ $\text{SiO}_2$  system.

#### 4. Conclusions

The stability of  $\text{CO}_2$  foams containing ionic surfactants and NPs in brine was evaluated for two oxide NPs with different surface charges at the low pH imposed by the dissolution of the gas in the aqueous phase. The results were compared with those of surfactant-only foams, and the impact of attractive or repulsive electrostatic interactions between surfactants and NPs on the interfacial and bulk rheological properties was discussed. The greater stability of the anionic and zwitterionic surfactants compared to that of the cationic surfactant was shown to be directly related to the efficiency of surfactant adsorption at the gas–solution interface, rather than to the CMC or to the surface excess. This indicates that interfacial elasticity plays an important role in these typically unstable  $\text{CO}_2$  foams. This trend was more evident in the presence of NPs in the systems, because a greater NP concentration was needed for a significant increase in  $t_{1/2}$  of foam with surfactants with higher  $pC_{20}$  values.

Surfactant/NP systems with attractive interactions under the experimental conditions (low pH and brine) also exhibited a significant increase in the bulk viscosity because

of the effect of inter-particle interactions in the solution which was mediated by the surfactants. However, we found that the most stable CO<sub>2</sub> foams were formed not only in systems with increased bulk viscosity (owing to inter-particle interactions in solution), but also when the NP adsorption at the bubble surface was higher, leading to interfacial films with lower mobility. In particular, the presence of positive and negative charges in the zwitterionic surfactant molecules allowed interactions with both NPs despite the different surface charges. A remarkable reduction in the initial drainage rate was observed for the CAPB/SiO<sub>2</sub> combination. This was due to the synergy of the effects of increasing bulk viscosity and interfacial rigidity/immobility, which reduced the coarsening rate and led to an increase in the CO<sub>2</sub> foam stability.

This study has shown that the use of NPs for applications involving CO<sub>2</sub> foam in brine should be tailored to decrease the early destabilisation mechanisms typical in these dispersions, where gas diffusion dominates the foam stability. Therefore, while foams based on surfactants with poor adsorption efficiency require low concentrations of oppositely charged NPs to significantly improve the foam  $t_{1/2}$  (by increasing bulk viscosity), a higher concentration of NPs is needed in the case of efficient foamers, since decreasing the mobility of the interfacial films due to NP interfacial adsorption is also needed for enhancing CO<sub>2</sub> foam stability. Further studies on how these interactions can influence CO<sub>2</sub> foam stability in porous media (where drainage has a secondary role compared to coarsening mechanisms) are needed to assess the advantages of using these systems in foam-based applications for EOR and carbon capture and storage.

**Supplementary Materials:** The following supporting information can be downloaded at: <https://www.mdpi.com/article/10.3390/colloids7010002/s1>, Table S1: pH of the surfactant/NPs combinations after CO<sub>2</sub> saturation; Table S2:  $\zeta$ -potentials of NPs in brine and surfactant solutions (standard deviation < 2 mV); Figure S1: Hydrodynamic diameter ( $D_H$ ) of (a) SiO<sub>2</sub> and (b) Al<sub>2</sub>O<sub>3</sub> NPs in brine and in CAPB solutions; Figure S2: Drainage curves of CO<sub>2</sub>-foams formed with (a) DTAB, (b) SDS, and (c) CAPB, in the absence and presence of NPs. Slope of the linear fits (red lines) represents the initial drainage rate ( $DR_i$ ).

**Author Contributions:** B.R.S.d.A.: Investigation, Conceptualisation, Methodology, Formal analysis, Writing—original draft. B.G.A.: Methodology, Conceptualisation, Writing—review and editing. A.M.P.: Conceptualisation, Supervision, Writing—review and editing. A.P.-G.: Conceptualisation, Writing—review and editing, Supervision, Project administration, Funding acquisition. All authors have read and agreed to the published version of the manuscript.

**Funding:** The current work was conducted in association with the R&D projects of ANP (Brazilian National Agency for Petroleum, Natural Gas and Biofuels) number 20358-8, “Desenvolvimento de formulações contendo surfactantes e nanopartículas para controle de mobilidade de gás usando espumas para recuperação avançada de petróleo” (PUC-Rio/Shell Brazil/ANP). It was funded by Shell Brazil, in partnership with Petrobras, and in accordance with ANP’s R&D regulations under the Research, Development, and Innovation Investment Commitment. This study was financed in part by the Coordenação de Aperfeiçoamento de Pessoal de Nível Superior (CAPES, Brazil)—Finance Code 001.

**Data Availability Statement:** Not applicable.

**Acknowledgments:** The authors would also like to thank Oxiteno Brazil for kindly providing the CAPB surfactant samples.

**Conflicts of Interest:** The authors declare no conflicts of interest. The funders had no role in the design of the study; in the collection, analyses, or interpretation of data; in the writing of the manuscript; or in the decision to publish the results.

## References

1. Farajzadeh, R.; Andrianov, A.; Bruining, H.; Zitha, P.L.J. Comparative study of CO<sub>2</sub> and N<sub>2</sub> foams in porous media at low and high pressure-temperatures. *Ind. Eng. Chem. Res.* **2009**, *48*, 4542–4552. <https://doi.org/10.1021/ie801760u>.
2. Aarra, M.G.; Skauge, A.; Solbakken, J.; Ormehaug, P.A. Properties of N<sub>2</sub>- and CO<sub>2</sub>-foams as a function of pressure. *J. Pet. Sci. Eng.* **2014**, *116*, 72–80. <https://doi.org/10.1016/j.petrol.2014.02.017>.

3. Zhou, Y.; Han, Z.; He, C.; Feng, Q.; Wang, K.; Wang, Y.; Luo, N.; Dodbiba, G.; Wei, Y.; Otsuki, A.; et al. Long-term stability of different kinds of gas nanobubbles in deionized and salt water. *Materials* **2021**, *14*, 1808. <https://doi.org/10.3390/ma14071808>.
4. Roberto, P.G.; Arturo, B.T. Coalescence of Air Bubbles: Effect of the electrical double layer. *Miner. Eng.* **2020**, *150*, 106301. <https://doi.org/10.1016/j.mineng.2020.106301>.
5. Worthen, A.; Bryant, S.; Huh, C.; Johnston, K. Carbon dioxide-in-water foams stabilized with nanoparticles and surfactant acting in synergy. *AIChE J.* **2013**, *59*, 3490–3501. <https://doi.org/10.1002/aic.14124>.
6. Binks, B.P. Particles as surfactants—Similarities and differences. *Curr. Opin. Colloid Interface Sci.* **2002**, *7*, 21–41. [https://doi.org/10.1016/S1359-0294\(02\)00008-0](https://doi.org/10.1016/S1359-0294(02)00008-0).
7. Guo, F.; Aryana, S. An experimental investigation of nanoparticle-stabilized CO<sub>2</sub> foam used in enhanced oil recovery. *Fuel* **2016**, *186*, 430–442. <https://doi.org/10.1016/j.fuel.2016.08.058>.
8. Emrani, A.S.; Nasr-El-Din, H.A. Stabilizing CO<sub>2</sub> foam by use of nanoparticles. *SPE J.* **2017**, *22*, 494–504. <https://doi.org/10.2118/174254-PA>.
9. Binks, B.P.; Horozov, T.S. Aqueous foams stabilized solely by silica nanoparticles. *Angew. Chem. Int. Ed.* **2005**, *44*, 3722–3725. <https://doi.org/10.1002/anie.200462470>.
10. Li, S.; Qiao, C.; Li, Z.; Wanambwa, S. Properties of carbon dioxide foam stabilized by hydrophilic nanoparticles and hexadecyltrimethylammonium bromide. *Energy Fuels* **2017**, *31*, 1478–1488. <https://doi.org/10.1021/acs.energyfuels.6b03130>.
11. Mohd, T.A.T.; Shukor, M.A.A.; Ghazali, N.A.; Alias, N.; Yahya, E.; Azizi, A.; Shahrudin, M.Z.; Ramleeh, N.A. Relationship between foamability and nanoparticle concentration of carbon dioxide (CO<sub>2</sub>) foam for enhanced oil recovery (EOR). *Appl. Mech. Mater.* **2014**, *548–549*, 67–71. <https://doi.org/10.4028/www.scientific.net/AMM.548-549.67>.
12. Mohd, T.A.T.; Muhayyidin, A.H.M.; Ghazali, N.A.; Shahrudin, M.Z.; Alias, N.; Arina, S.; Ismail, S.N.; Ramlee, N.A. Carbon dioxide (CO<sub>2</sub>) foam stability dependence on nanoparticle concentration for enhanced oil recovery (EOR). *Appl. Mech. Mater.* **2014**, *548–549*, 1876–1880. <https://doi.org/10.4028/www.scientific.net/AMM.548-549.1876>.
13. Murshed, S.M.S.; Estellé, P. A state of the art review on viscosity of nanofluids. *Renew. Sustain. Energy Rev.* **2017**, *76*, 1134–1152. <https://doi.org/10.1016/j.rser.2017.03.113>.
14. Ab Rasid, S.A.; Mahmood, S.M.; Kechut, N.I.; Akbari, S. A review on parameters affecting nanoparticles stabilized foam performance based on recent analyses. *J. Pet. Sci. Eng.* **2022**, *208*, 109475. <https://doi.org/10.1016/j.petrol.2021.109475>.
15. Yekeen, N.; Idris, A.K.; Manan, M.A.; Samin, A.M. Experimental study of the influence of silica nanoparticles on the bulk stability of SDS-Foam in the presence of oil. *J. Dispers. Sci. Technol.* **2017**, *38*, 416–424. <https://doi.org/10.1080/01932691.2016.1172969>.
16. Yekeen, N.; Padmanabhan, E.; Idris, A.K. Synergistic effects of nanoparticles and surfactants on n-decane-water interfacial tension and bulk foam stability at high temperature. *J. Pet. Sci. Eng.* **2019**, *179*, 814–830. <https://doi.org/10.1016/j.petrol.2019.04.109>.
17. Zargartalebi, M.; Kharrat, R.; Barati, N. Enhancement of surfactant flooding performance by the use of silica nanoparticles. *Fuel* **2015**, *143*, 21–27. <https://doi.org/10.1016/j.fuel.2014.11.040>.
18. Vatanparast, H.; Samiee, A.; Bahramian, A.; Javadi, A. Surface behavior of hydrophilic silica nanoparticle-SDS surfactant solutions: I. Effect of nanoparticle concentration on foamability and foam stability. *Coll. Surfaces A Physicochem. Eng. Asp.* **2017**, *513*, 430–441. <https://doi.org/10.1016/j.colsurfa.2016.11.012>.
19. Zhao, J.; Torabi, F.; Yang, J. The synergistic role of silica nanoparticle and anionic surfactant on the static and dynamic CO<sub>2</sub> foam stability for enhanced heavy oil recovery: An experimental study. *Fuel* **2021**, *287*, 119443. <https://doi.org/10.1016/j.fuel.2020.119443>.
20. Ma, L.; Zhu, M.; Liu, T. Effects of chain length of surfactants and their adsorption on nanoparticles on stability of CO<sub>2</sub>-in-water emulsions. *Coll. Surfaces A Physicochem. Eng. Asp.* **2022**, *644*, 128877. <https://doi.org/10.1016/j.colsurfa.2022.128877>.
21. Yekeen, N.; Manan, M.A.; Idris, A.K.; Padmanabhan, E.; Junin, R.; Samin, A.M.; Gbadamosi, A.O.; Oguamah, I. A comprehensive review of experimental studies of nanoparticles-stabilized foam for enhanced oil recovery. *J. Pet. Sci. Eng.* **2018**, *164*, 43–74. <https://doi.org/10.1016/j.petrol.2018.01.035>.
22. Farhadi, H.; Riahi, S.; Ayatollahi, S.; Ahmadi, H. Experimental study of nanoparticle-surfactant-stabilized CO<sub>2</sub> foam: Stability and mobility control. *Chem. Eng. Res. Des.* **2016**, *111*, 449–460. <https://doi.org/10.1016/j.cherd.2016.05.024>.
23. Marčelja, S.; Lu, H.; Yuan, M.; Fang, B.; Wang, J.; Guo, Y.; Roberto, P.G.; Arturo, B.T.; Johnson, S.B.; Franks, G.V.; et al. Wormlike micelles in mixed amino acid-based anionic surfactant and zwitterionic surfactant systems. *Langmuir* **2018**, *14*, 8061–8074. <https://doi.org/10.1039/c8sm01949e>.
24. Lewis, J.A. Colloidal processing of ceramics. *Adv. Appl. Ceram.* **2004**, *83*, 2341–2359. <https://doi.org/10.1111/j.1151-2916.2000.tb01560.x>.
25. Drexler, S.; Silveira, T.M.G.; De Belli, G.; Couto, P. Experimental study of the effect of carbonated brine on wettability and oil displacement for EOR application in the Brazilian pre-salt reservoirs. *Energy Sources Part A Recover. Util. Environ. Eff.* **2021**, *43*, 3282–3296. <https://doi.org/10.1080/15567036.2019.1604877>.
26. Rosen, M.J.; Kunjappu, J.T. *Surfactants and Interfacial Phenomena*; John Wiley & Sons, Inc.: Hoboken, NJ, USA, 2012. <https://doi.org/10.1002/9781118228920>.
27. Wang, C.; Fang, H.; Gong, Q.; Xu, Z.; Liu, Z.; Zhang, L.; Zhang, L.; Zhao, S. Roles of catanionic surfactant mixtures on the stability of foams in the presence of oil. *Energy Fuels* **2016**, *30*, 6355–6364. <https://doi.org/10.1021/acs.energyfuels.6b01112>.
28. Petkova, B.; Tcholakova, S.; Chenkova, M.; Golemanov, K.; Denkov, N.; Thorley, D.; Stoyanov, S. Foamability of aqueous solutions: Role of surfactant type and concentration. *Adv. Colloid Interface Sci.* **2020**, *276*, 102084. <https://doi.org/10.1016/j.cis.2019.102084>.



29. Wang, L.; Yoon, R. Effects of surface forces and film elasticity on foam stability. *Int. J. Miner. Process.* **2008**, *85*, 101–110. <https://doi.org/10.1016/j.minpro.2007.08.009>.
30. Hu, N.; Li, Y.; Wu, Z.; Lu, K.; Huang, D.; Liu, W. Foams stabilization by silica nanoparticle with cationic and anionic surfactants in column flotation: Effects of particle size. *J. Taiwan Inst. Chem. Eng.* **2018**, *88*, 62–69. <https://doi.org/10.1016/j.jtice.2018.04.008>.
31. Wang, W.; Gu, B.; Liang, L. Effect of Surfactants on the formation, morphology, and surface property of synthesized SiO<sub>2</sub> nanoparticles. *J. Dispers. Sci. Technol.* **2005**, *25*, 593–601. <https://doi.org/10.1081/DIS-200027309>.
32. Muhamad, M.S.; Salim, M.R.; Lau, W.-J. Surface modification of SiO<sub>2</sub> nanoparticles and its impact on the properties of PES-based hollow fiber membrane. *RSC Adv.* **2015**, *5*, 58644–58654. <https://doi.org/10.1039/C5RA07527K>.
33. Yekeen, N.; Idris, A.K.; Manan, M.A.; Samin, A.M.; Risal, A.R.; Kun, T.X. Bulk and bubble-scale experimental studies of influence of nanoparticles on foam stability. *Chin. J. Chem. Eng.* **2017**, *25*, 347–357. <https://doi.org/10.1016/j.cjche.2016.08.012>.
34. Rezaei, A.; Derikvand, Z.; Parsaei, R.; Imanivarnosfaderani, M. Surfactant-silica nanoparticle stabilized N<sub>2</sub>-foam flooding: A mechanistic study on the effect of surfactant type and temperature. *J. Mol. Liq.* **2021**, *325*, 115091. <https://doi.org/10.1016/j.molliq.2020.115091>.
35. Aladag, B.; Halelfadl, S.; Doner, N.; Maré, T.; Duret, S.; Estellé, P. Experimental investigations of the viscosity of nanofluids at low temperatures. *Appl. Energy* **2012**, *97*, 876–880. <https://doi.org/10.1016/j.apenergy.2011.12.101>.
36. Safouane, M.; Saint-Jalmes, A.; Bergeron, V.; Langevin, D. Viscosity effects in foam drainage: Newtonian and non-Newtonian foaming fluids. *Eur. Phys. J. E* **2006**, *19*, 195–202. <https://doi.org/10.1140/epje/e2006-00025-4>.
37. Creatto, E.J.; Alvarenga, B.G.; de Moura, P.G.; Pérez-Gramatges, A. Viscosity-driven stabilization of CO<sub>2</sub>-in-brine foams using mixtures of cocamidopropyl hydroxysultaine and sodium dodecyl sulfate. *J. Mol. Liq.* **2021**, *329*, 115614. <https://doi.org/10.1016/j.molliq.2021.115614>.
38. Alvarenga, B.G.; Gonçalves, C.C.R.; Pérez-Gramatges, A. Stabilization of CO<sub>2</sub>-foams in brine by reducing drainage and coarsening using alkyldimethylamine oxides as surfactants. *J. Mol. Liq.* **2022**, *347*, 118370. <https://doi.org/10.1016/j.molliq.2021.118370>.
39. Wang, Z.; Ren, G.; Yang, J.; Xu, Z.; Sun, D. CO<sub>2</sub>-Responsive aqueous foams stabilized by pseudogemini surfactants. *J. Colloid Interface Sci.* **2019**, *536*, 381–388. <https://doi.org/10.1016/j.jcis.2018.10.040>.
40. Da, C.; Jian, G.; Alzobaidi, S.; Yang, J.; Biswal, S.L.; Hirasaki, G.J.; Johnston, K.P. Design of CO<sub>2</sub>-in-water foam stabilized with switchable amine surfactants at high temperature in high-salinity brine and effect of oil. *Energy Fuels* **2018**, *32*, 12259–12267. <https://doi.org/10.1021/acs.energyfuels.8b02959>.
41. Xue, Z.; Worthen, A.; Qajar, A.; Robert, I.; Bryant, S.L.; Huh, C.; Prodanović, M.; Johnston, K.P. Viscosity and stability of ultra-high internal phase CO<sub>2</sub>-in-water foams stabilized with surfactants and nanoparticles with or without polyelectrolytes. *J. Coll. Interface Sci.* **2016**, *461*, 383–395. <https://doi.org/10.1016/j.jcis.2015.08.031>.
42. Ravera, F.; Santini, E.; Loglio, G.; Ferrari, M.; Liggieri, L. Effect of nanoparticles on the interfacial properties of liquid/liquid and liquid/air surface layers. *J. Phys. Chem. B* **2006**, *110*, 19543–19551. <https://doi.org/10.1021/jp0636468>.
43. Romero, C.P.; Jeldres, R.I.; Quezada, G.R.; Concha, F.; Toledo, P.G. Zeta potential and viscosity of colloidal silica suspensions: Effect of seawater salts, PH, flocculant, and shear rate. *Colloids Surfaces A Physicochem. Eng. Asp.* **2018**, *538*, 210–218. <https://doi.org/10.1016/j.colsurfa.2017.10.080>.
44. Majumder, S.; Naskar, B.; Ghosh, S.; Lee, C.H.; Chang, C.H.; Moulik, S.P.; Panda, A.K. Synthesis and characterization of surfactant stabilized nanocolloidal dispersion of silver chloride in aqueous medium. *Coll. Surfaces A Physicochem. Eng. Asp.* **2014**, *443*, 156–163. <https://doi.org/10.1016/j.colsurfa.2013.10.064>.
45. Skoglund, S.; Blomberg, E.; Wallinder, I.O.; Grillo, I.; Pedersen, J.S.; Bergström, L.M. A novel explanation for the enhanced colloidal stability of silver nanoparticles in the presence of an oppositely charged surfactant. *Phys. Chem. Chem. Phys.* **2017**, *19*, 28037–28043. <https://doi.org/10.1039/c7cp04662f>.
46. Horozov, T.S. Foams and foam films stabilised by solid particles. *Curr. Opin. Coll. Interface Sci.* **2008**, *13*, 134–140. <https://doi.org/10.1016/J.COCIS.2007.11.009>.
47. Varade, D.; Carriere, D.; Arriaga, L.R.; Fameau, A.L.; Rio, E.; Langevin, D.; Drenckhan, W. On the origin of the stability of foams made from catanionic surfactant mixtures. *Soft Matter* **2011**, *7*, 6557–6570. <https://doi.org/10.1039/c1sm05374d>.
48. Saint-Jalmes, A. Physical chemistry in foam drainage and coarsening. *Soft Matter* **2006**, *2*, 836–849. <https://doi.org/10.1039/b606780h>.
49. Wang, J.; Nguyen, A.V.; Farrokhpay, S. A critical review of the growth, drainage and collapse of foams. *Adv. Coll. Interface Sci.* **2016**, *228*, 55–70. <https://doi.org/10.1016/j.cis.2015.11.009>.
50. Koehler, S.A.; Hilgenfeldt, S.; Stone, H.A. Generalized view of foam drainage: Experiment and theory. *Langmuir* **2000**, *16*, 6327–6341. <https://doi.org/10.1021/la9913147>.
51. Saint-Jalmes, A.; Langevin, D. Time evolution of aqueous foams: Drainage and coarsening. *J. Phys. Condens. Matter* **2002**, *14*, 9397–9412. <https://doi.org/10.1088/0953-8984/14/40/325>.

**Disclaimer/Publisher’s Note:** The statements, opinions and data contained in all publications are solely those of the individual author(s) and contributor(s) and not of MDPI and/or the editor(s). MDPI and/or the editor(s) disclaim responsibility for any injury to people or property resulting from any ideas, methods, instructions or products referred to in the content.